Flat Surface Reconstruction Using Sonar

Thomas C. Henderson, Mohamed Dekhil, Beat Brüderlin,
Larry Schenkat and Larkin Veigel[1]

UUSC-96-003

Department of Computer Science
University of Utah
Salt Lake City, UT 84112 USA

March 1996

Abstract

A technique is given for the recovery of planar surfaces using two beam-spread sonar readings. If a single, planar surface gave rise to the two readings, then the method recovers the surface quite accurately. Simulation and experiment demonstrate the effectiveness of the technique and recommend its use in practice.

[1]This work was supported in part by the Advanced Research Projects agency under Army Research Office grants number DAAH04-93-G-0420 and by NSF grant CDA 9024721.

Flat Surface Reconstruction Using Sonar

Thomas C. Henderson, Mohamed Dekhil, Beat Brüderlin,
Larry Schenkat and Larkin Veigel

Department of Computer Science
University of Utah
Salt Lake City, Utah 84112, USA

Abstract

A technique is given for the recovery of planar surfaces using two beam-spread sonar readings. If a single, planar surface gave rise to the two readings, then the method recovers the surface quite accurately. Simulation and experiment demonstrate the effectiveness of the technique and recommend its use in practice.

1 Introduction

Sonar sensors in common use today (e.g., the Polaroid sensor) produce with reasonable accuracy the range to the nearest surface, but the direction to that surface is not explicitly determined; rather the surface is known to lie within a certain angle spread centered about the line of direction of the sensor (e.g., 22.5° for the Polaroid sensor). (See Figure 1.) Multiple sonar readings are required to disambiguate

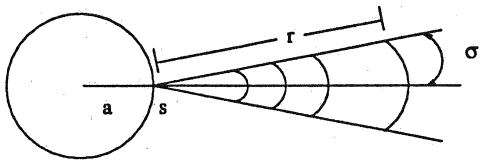

Figure 1: Beamspread of Sonar Sensor

the location (pose) of the reflecting surface. Several researchers have investigated the use of sonar in mobile robotics [Bozma and Kuc, 1991, Crowley, 1985, Elfes, 1987, Leonard and Durrant-Whyte, 1991, Matthies and Elfes, 1988], and others have directly addressed the problem of wall detection

This work was supported in part by the Advanced Research Projects agency under Army Research Office grants number DAAH04-93-G-0420 and by NSF grant CDA 9024721.

[Bozma and Kuc, 1990, Borenstein and Koren, 1995, Kleeman and Kuc, 1995, Peremans *et al.*, 1993], or have shown the minimum number and arrangement of sonar sensors to detect obstacles [Kuc, 1990, Kuc, 1991]. However, no one has addressed the optimal pose recovery of planar surfaces in sonar data (see [Henderson *et al.*, 1996a, Henderson *et al.*, 1996b]). In this paper, we address the simplest version of the k-wall/m-sonar (kWmS) problem:

> **Problem:** Given m sonar transmitter/receiver sensors situated on a circular ring placed in a k wall enclosure, what is the optimal sensing strategy to determine the pose of the k walls?

The sonar sensor is assumed to have a non-zero beam spread (e.g., 22.5 degrees for a Polaroid sensor), and optimal is defined in terms of the recovery of the wall's pose with the minimum number of sensors used and moves made.

We start with the recovery of a single wall in the sensor's field of view. Given a single sonar sensor located on a circular ring at a distance a from the center of the ring, we show that two sonar readings, with one sensing position rotated with respect to the other (with certain conditions on the angle of rotation), suffice to recover the pose of a wall. This reduces to a plane geometry problem in which the wall is represented as a line in the plane, and its equation is determined.

2 Pose Determination of Wall

Assume that the environment consists of a single wall whose pose is to be determined (i.e., a line in the plane). There are three key insights:

1. a single sonar reading determines a set, S, of possible lines,
2. for the spread-beam sonar, S is qualitatively different from a narrow-beam sonar, and
3. if correctly positioned, a second sonar reading can disambiguate which line in S gave rise to the two readings.

Figure 2 compares the broad-beam and narrow-beam line sets. For a narrow-beam sensor, only the orientation of the line is unknown, whereas for a broad-beam sensor there are many possible positions and orientations of the line. Under certain conditions there is a one-to-one relation between the second sonar reading and the lines in S. Figure 3 shows a sample set of lines for $a = 1$ and $r = 2$, while Figure 4 shows the sonar distance from a second sonar (rotated $-\pi/6$ from the first) to each of these lines; as can be seen, the plot of distance decreases monotonically and this makes it possible to use the second sonar range to ascertain the line that gave rise to the two readings.

Suppose we are given a single sonar located at s on a circular platform of radius a as shown in Figure 1, and that it indicates a return at range r. The sensor is assumed to have a beam spread 2σ, and to reflect back a signal incident to a surface at any angle (the fact that there is in practice a minimum

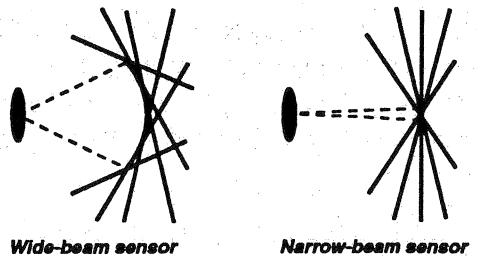

Figure 2: Broad- and Narrow-beam Line Set Comparison

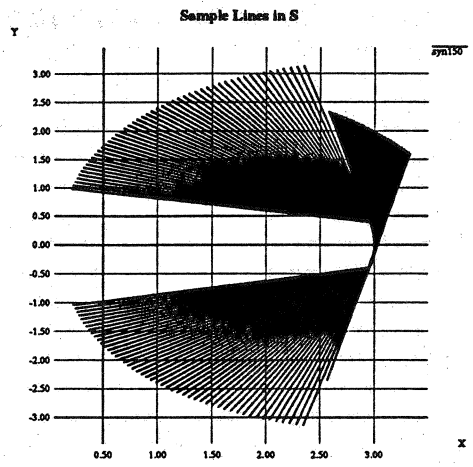

Figure 3: Set of Possible Lines

incident angle that gives a reflection will be accounted for later). Furthermore, assume that there is only one wall in the vicinity of the sonar and it reflects a signal (i.e., it intersects the sonar wedge).

Then Figure 5 shows the three qualitatively different sets of possible lines that could have produced a range reading of r. The qualitative line sets are:

1. $S1$: The set of lines found by rotating l_0 about E into l_i.
2. $S2$: The set of lines found by sliding the tangent line along the circular arc EF from l_i to l_j.
3. $S3$: The set of lines found by rotating l_j about F into l_m.

We will show that the line which caused the range return value of r can be disambiguated by taking one more sonar reading after rotating the sonar sensor about the origin by an amount less than $\angle AEC$ (call that angle α) to the new position B. The sonar range distances from B to the lines in sets $S1$, $S2$, and $S3$ are monotonically decreasing, which permits a simple determination of the line that produced

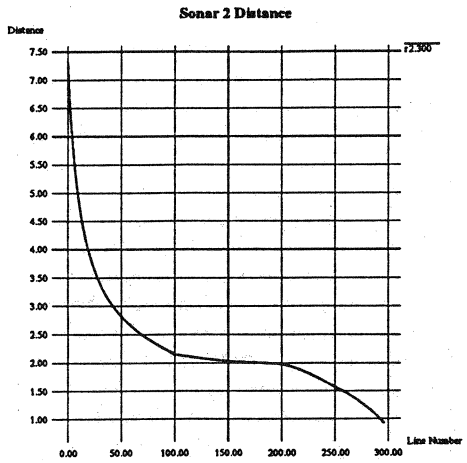

Figure 4: Distance from Second Sonar to Possible Lines

r (in fact, the discontinuities between the range to lines in S_1 and lines in S_2 can be seen at line 100 in Figure 4 and at line 200 for lines in S_2 and S_3).

Now, consider a clockwise rotation of angle θ of the sonar located at A rotated about O from A to B where $0 < \theta < \alpha$ (see Figure 6). Any ray in the second sonar scan to the right of l_l will intersect all lines in $S1$ at a greater distance than l_l will. In addition, the distance along l_l monotonically decreases to a line l as it starts at line l_0 and is rotated about E to line l_i. To see this, drop a perpendicular from E to segment $\overline{HG}$ of height $h = d \times \sin(\beta)$ (where $d = \mid \overline{EH} \mid$, and β is $\angle EHG$). It is clear that as segment $\overline{EG}$ rotates clockwise around E, segment $\overline{HI}$ goes monotonically to length zero, where point I is the intersection of lines l_i and l. (Note that the perpendicular to l_l through E is past l_i.) This follows from the fact that if $b = \mid \overline{HI} \mid$, then the area of triangle $\triangle EHI$ monotonically decreases, so that $\frac{1}{2}bh$ does, too, which implies that b does since h is constant.

We now show under what conditions the second sonar distance function is invertible. Consider the circle C_1 shown in Figure 7 with the point C the location of the first sonar reading. Given a point, P, in the circle not at the center, C, then the shortest distance from P to a tangent line to C_1 achieves a maximum at A, and a minimum to a tangent of the circle at B. This distance monotonically decreases for the tangent lines at points on C_1 as they range from A to B.

Now, we prove that the distance from the second sonar to the tangent lines along the arc AB decreases monotonically. Suppose not; then there exist two points D_1 and D_2 on the circle between A and B such that P is equidistant from the tangent lines to circle C_1 at D_1 and D_2 (i.e., $|PE_1| = |PE_2|$ where E_1 and E_2 are the points of intersection of the perpendiculars to the tangent lines at D_1 and D_2, respectively.) Consider the two triangles PE_1F and PE_2F, we have:

$$\overline{PF}^2 = \overline{PE_1}^2 + \overline{E_1F}^2 = \overline{PE_2}^2 + \overline{E_2F}^2 \quad (1)$$

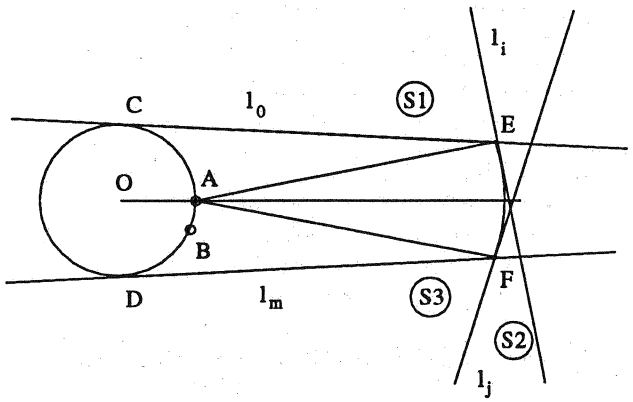

Figure 5: Qualitative Line Sets

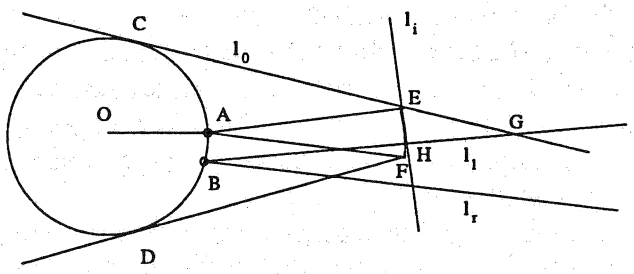

Figure 6: Set 1 Distances

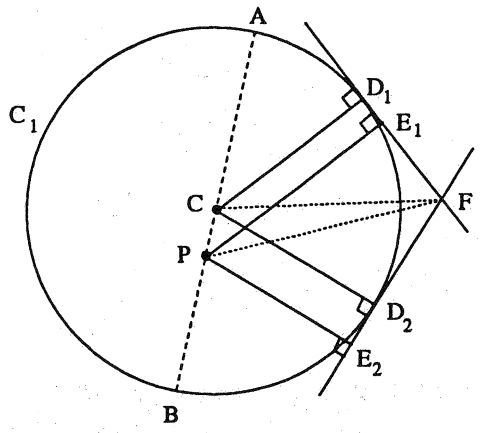

Figure 7: Distance from P to the tangent lines (Set 2 lines).

From the assumption that $|\overline{PE_1}| = |\overline{PE_2}|$ and Equation 1, we have:

$$|\overline{E_1F}| = |\overline{E_2F}| \tag{2}$$

From the two triangles CD_1F and CD_2F, since $|\overline{CD_1}|$ and $|\overline{CD_2}|$ are equal (both equal to the radius of the circle C_1,) and since $\overline{CF}$ is a common side in both triangles, therefore,

$$|\overline{D_1F}| = |\overline{D_2F}| \tag{3}$$

Also, from Figure 7, we can see that

$$|\overline{E_1F}| = |\overline{D_1F}| - |\overline{D_1E_1}| \tag{4}$$

and

$$|\overline{E_2F}| = |\overline{D_2F}| + |\overline{E_2D_2}| \tag{5}$$

Combining Equations 2,3,4,5 we get:

$$|\overline{D_1E_1}| + |\overline{E_2D_2}| = 0 \tag{6}$$

which means that $|\overline{D_1E_1}| = 0$ and $|\overline{D_2E_2}| = 0$, and so the two points E_1 and E_2 coincides with the two points D_1 and D_2, respectively. And since $\overline{PE_1}$ and $\overline{PE_2}$ are perpendiculars to the tangent lines of circle C_1, then P must coincide with the center of the circle, C, which contradicts the condition that P should be a point not at the center of the circle C_1.

Now, for the final set of lines, $S3$, we consider two subsets (see Figure 8). Let l_k be the line between l_j and l_m which is perpendicular to l_r. Then, for all lines between l_k and l_m, as l_k is rotated around F to l_m, the shortest distance from B to the line is along a line clockwise from l_r; therefore, for those lines the shortest distance in the sonar wedge from B is along line l_r and monotonically decreases.

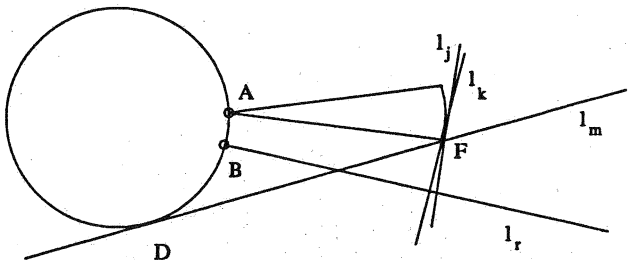

Figure 8: Set 3 Distances

Finally, for the lines from l_j to l_k, we claim that the shortest distance from B decreases monotonically. Suppose not. Then there exist two points J_1 and J_2 such that the distance d to B is the same. Since for this set of lines, the shortest distance is on the perpendicular to B, then there exist two tangent lines to the circle centered at B of radius d such that both lines go through F and are on the same side of the circle. $\otimes$

Thus, we have shown that given the set of lines that could cause a sonar return of r from a single wall, then a second sonar return from a rotated location is sufficient to disambiguate the pose of the wall. However, the proof has imposed two conditions on the rotated position:

- The angle between the first and second sonar locations cannot exceed α, the angle between the lines l_0 and $\overleftrightarrow{AE}$ (Figure 6).
- The line $\overleftrightarrow{BA}$ (Figure 7) should not cut the arc EF (Figure 6).

To see that this solves the wall pose recovery problem, note that so long as the sonar sensor is rotated a non-zero amount about the center of the non-zero radius sonar ring, but less than the angle made by a tangent to the robot that goes through the sector corners, then the proof applies and the pose of the wall can be found. C and P play the roles of the first and second sonar locations, respectively.

3 An Implementation

Given two sonar readings r_1 and r_2, we can determine the pose of the wall, assuming that the wall is flat and in the field of view of both sensors. First, let's define some points as shown in Figure 9. Two sensors are located on a circular arc at locations S_1^c and S_2^c with fields of view represented by the two sectors S_1 and S_2, respectively. The corners of each sector are defined by the points S_i^+ and S_i^- as shown in Figure 9.

A simple solution is to use bisection search on the set of lines to find the line at (sonar) distance r_2 from S_2^c.

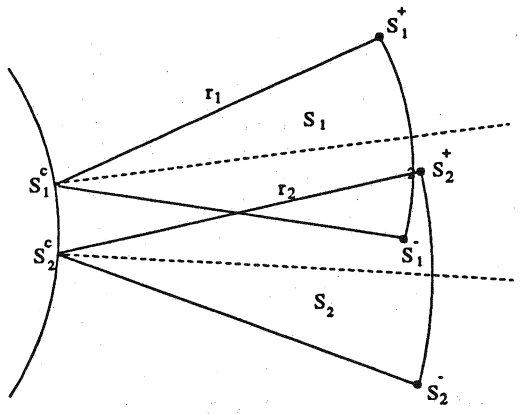

Figure 9: Notation used in the algorithm.

Another approach is to separate the line set into qualitatively distinct categories. There are five different cases for the orientation of the wall with respect to the two sensors. These cases are shown in Figures 10 through 14 and can be summarized as follows:

Case I: the wall is tangent to neither sector arc and goes through S_1^+ and S_2^+.

Case II: the wall is tangent to S_1 but not to S_2 and goes through S_2^+.

Case III: the wall is tangent to both arcs of S_1 and S_2.

Case IV: the wall is tangent to S_2 but not to S_1 and goes through S_1^-.

Case V: the wall is tangent to neither sector arc and goes through S_1^- and S_2^-.

For each of these cases, by fixing r_1, the value of r_2 can determine which region the wall is in. The following algorithm can be used to determine the wall pose given the two sensor readings r_1 and r_2.

- if $r_1 \leq r_2$ then
  1. draw a tangent line from point S_1^+ to the arc of sector S_1 (see Figure 10).
  2. if the distance from point S_2^c to that tangent along the line $\overline{S_2^c S_2^+}$ is less than or equal r_2, then the wall is in the first region, and it is represented by the line segment connecting S_1^+ and S_2^+.
  3. else, draw a tangent to the arc of sector S_2 from point S_2^+, as shown in Figure 11.

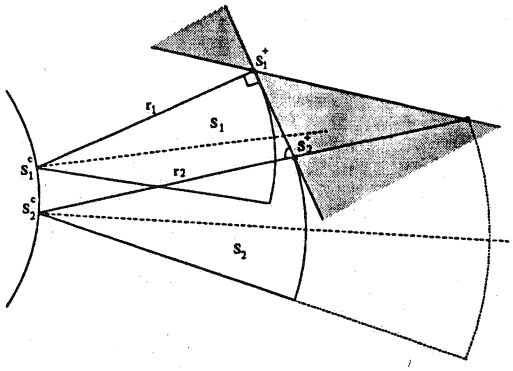

Figure 10: First region.

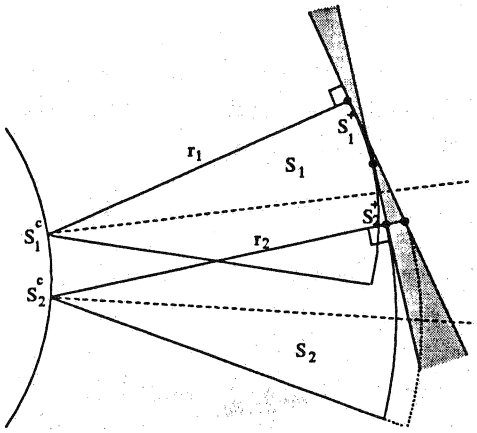

Figure 11: Second region.

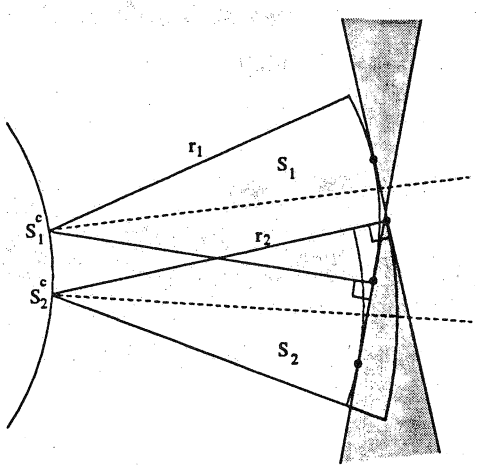

Figure 12: Third region.

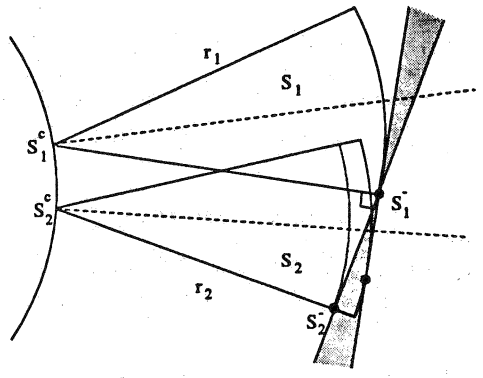

Figure 13: Fourth region.

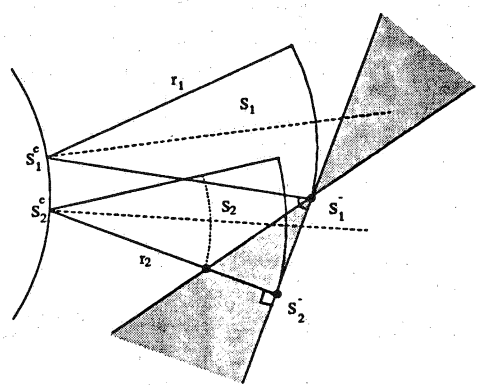

Figure 14: Fifth region.

4. if the distance from the point S_1^c to that tangent is greater than or equal r_1, then the wall is in the second region and the tangent to sector S_1 which goes through S_2^+ represents the wall.
5. else, the wall is in the third region (Figure 12), and is represented by the common tangent to the two arcs.

- else if $r_1 > r_2$ then

1. draw a tangent line from point S_2^- to the arc of the sensor at S_2 (see Figure 14).
2. if the distance from point S_1^c to that tangent along the line $\overline{S_1^c S_1^-}$ is less than or equal r_1, then the wall is in the fifth region, and it is represented by the line segment connecting S_1^- and S_2^-.
3. else, draw a tangent to the arc of sector S_1 from point S_1^-, as shown in Figure 13.
4. if the distance from the point S_2^c to that tangent is greater than or equal r_2, then the wall is in the fourth region and the tangent to sector S_2 which goes through S_1^- represents the wall.
5. else, the wall is in the third region (Figure 12), and is represented by the common tangent to the two arcs.

Now, the only thing left is to find the common tangent to two circles. Figure 15 shows the basic idea of finding the common tangent. By connecting the two centers, C and P, and extending the line segment $\overline{CP}$ to F where the distance $|\overline{PF}|$ can be calculated from the equality:

$$\frac{r_1}{r_2} = \frac{|\overline{FC}|}{|\overline{FP}|} \tag{7}$$

where

$$|\overline{FC}| = |\overline{FP}| - |\overline{CP}| \tag{8}$$

From point F, we draw a line that makes an angle of θ with the line $\overline{FP}$ where

$$\sin\theta = \frac{|r_2 - r_1|}{|\overline{CP}|} \tag{9}$$

4 Experimental Results

In practice, sonar sensors located on a ring and with at most 18° difference in their directions can be used pairwise to recover hypotheses about walls present in the environment (this is due to the fact that a sonar/wall incident angle of greater than 60 degrees is necessary to get a return). We present here

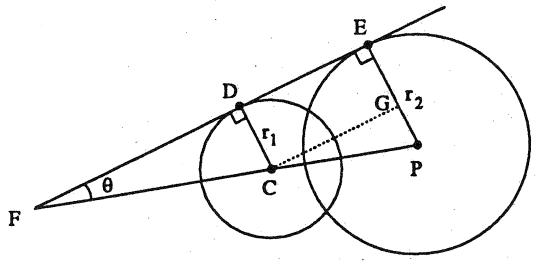

Figure 15: Finding the Common Tangent of Two Circles.

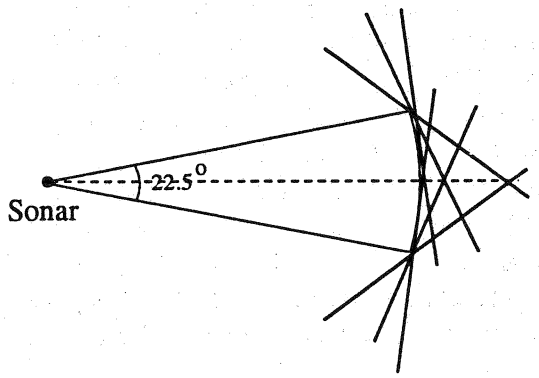

Figure 16: Reference Wall Experiment

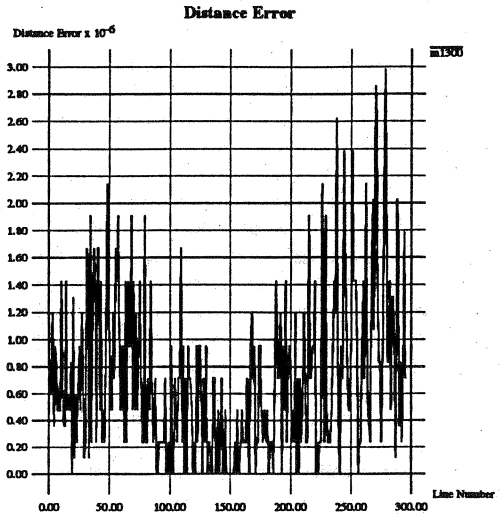

Figure 17: Synthetic Data: Distance

some experimental data taken with walls located in known positions with respect to the sonar ring and compare the calculated poses.

First, we consider the setup shown in Figure 16.

A simulation of this set up results in the error curves shown in Figure 17 (distance) and Figure 18 (angle). This error is a result of numerical round-off error.

In the actual experiment, a wall (a large modular office partition wall) was placed at a fixed distance, d, but at various tangents to the circle of radius d centered at the sonar sensor, S_1. A reading is then taken from the second sonar sensor, S_2, and the pose calculated. Figure 19 shows the range reading from a central sonar and two side sonars and clearly indicates the stability of the range of the central sonar and the monotonic nature of the two side sonars.

Next, we repeat this experiment, but with the robot interacting with actual walls in an office. The pose of the walls was determined by measurement with the center of the sonar ring the origin, and the forward facing sonar of the robot giving the x-axis. Figure 20 shows the the angle error between the computed wall orientation and the actual wall orientation. Figure 21 shows the the distance error between the computed wall and the actual wall (where distance is the normal distance from the origin to the wall).

In addition, we compared our method with a more standard approximation used in the mobile robot community. A pose estimate can be made by assuming there is no beam spread on the sonar so that two distinct points on the wall are given by the orientation and range of the two sonar readings. The line is then defined by these two points. A comparison of the error in this method and the error in our method is given in Figures 22 and 23.

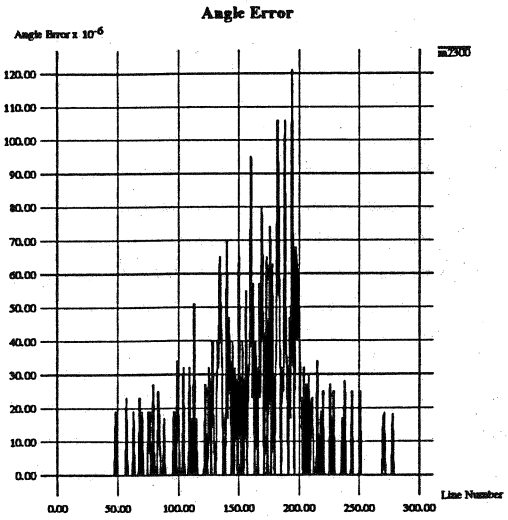

Figure 18: Synthetic Data: Orientation

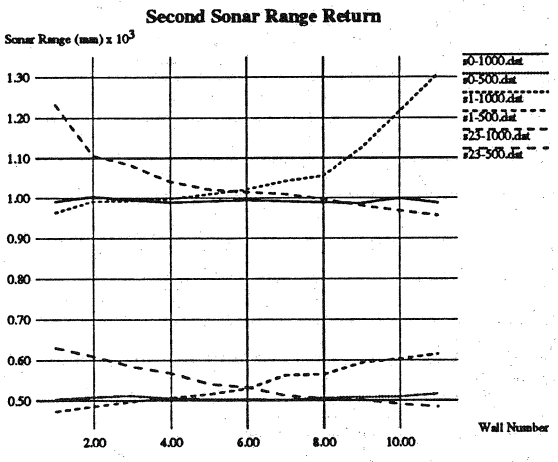

Figure 19: Controlled Line Recovery Data

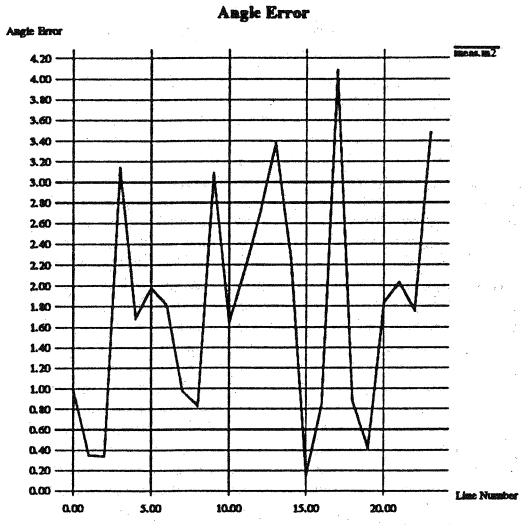

Figure 20: Experimental Data: Orientation

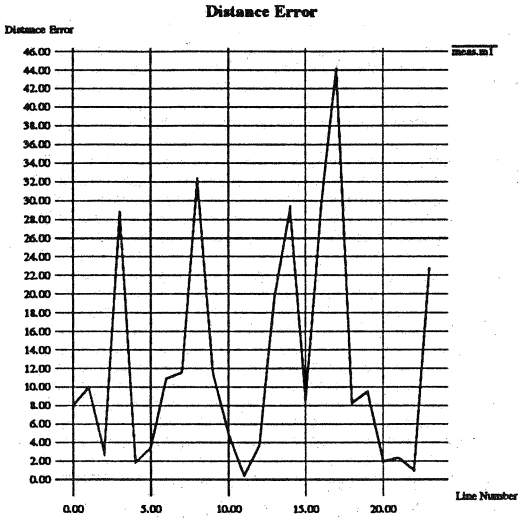

Figure 21: Experimental Data: Distance

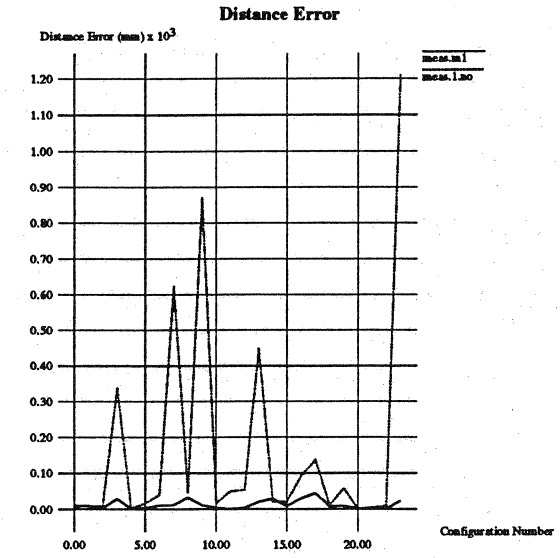

Figure 22: Method Comparison: Distance

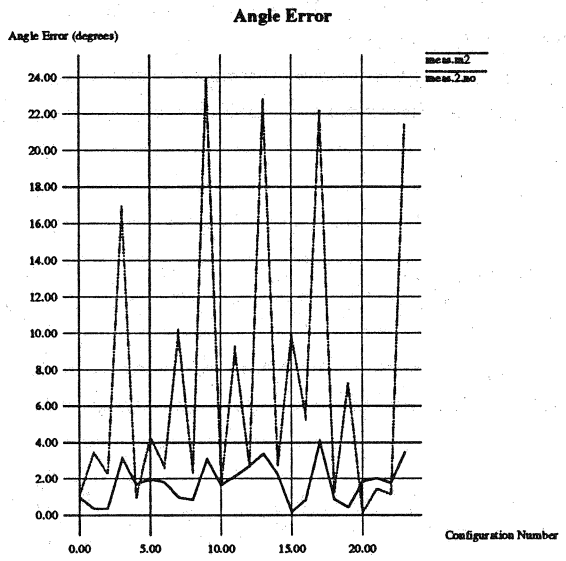

Figure 23: Method Comparison: Orientation

5 Conclusions

An optimal sonar sensing strategy is given for the use of two sonar readings for the recovery of wall positions in the environment. This technique can be used to generate hypotheses of wall surfaces which helps define precise strategies to take more data which corroborate or disconfirm the hypotheses. The underlying geometrical arguments may also be relevant to other kinds of sensors with similar beam spread physics.

We have presented a solution to the 1W1S problem, and believe that it is optimal. We have demonstrated its effectiveness on synthetic data, and on actual Polaroid sonar data. We have shown that the line estimates for two range sensor readings produced by this method are better than using line estimates from the two points obtained simply from using the sensor orientation and range in that direction (as suggested by e.g., see[Kuc, 1990]: "A sonar map is generated by placing a dot at the computer range along the transducer orientation").

The error in the actual data is due to both the error in the range readings and the numerical error involved in the computation. The minimum incident angle does not need to be accounted for since the method only produces a flat surface hypothesis for two neighboring sonar sensors that both produce a range value. For more details see[Henderson *et al.*, 1996a].

Given that the smallest angle that gives a sonar return is about 60 degrees, it is necessary to have at least 20 sonar sensors equally spaced and no more than 18 degrees apart in order to be able to detect a wall within sonar range of a mobile platform (also see [Kuc, 1991]). Our particular Labmate has a 24 sonar ring with sensors spaced 15 degrees apart and was used for the experiments described here. The idea is that this method permits the hypothesis on any possible walls, and then those hypotheses can be checked out by moving and taking more readings.

We are also studying the kWmS problem in more generality. We believe that the equations and specific constraints can be solved in the multiple wall, multiple sonar case as well.

References

[Borenstein and Koren, 1995] J. Borenstein and Y. Koren. Error eliminating rapid ultrasonic firing mobile robot obstacle avoidance. *IEEE Journal of Robotics and Automation*, 11:132–138, 1995.

[Bozma and Kuc, 1990] B. Bozma and R. Kuc. Differentiating sonar reflections from corners and planes by employing an intelligent sensor. *IEEE Trans. Pattern Analysis and Machine Intelligence*, 12(6):pp. 560–569, June 1990.

[Bozma and Kuc, 1991] O. Bozma and R. Kuc. Building a sonar map in a specular environment using a single mobile sensor. *IEEE Trans. Pattern Analysis and Machine Intelligence*, 13(12):pp. 1260–1269, December 1991.

[Crowley, 1985] J. Crowley. Navigation for an intelligent robot. *IEEE Journal of Robotics and Automation*, RA-1(1):pp. 31–41, March 1985.

[Elfes, 1987] A. Elfes. Sonar-based real-world modeling and navigation. *IEEE Trans. Robotics and Automation*, RA-3(3):pp. 249–265, June 1987.

[Henderson *et al.*, 1996a] Thomas C. Henderson, Beat Bruderlin, Mohamed Dekhil, Larry Schenkat, and Larkin Veigel. Sonar sensing strategies. In *IEEE Int. Conf. Robotics and Automation*, page to appear, 1996.

[Henderson *et al.*, 1996b] Thomas C. Henderson, Mohamed Dekhil, Beat Bruderlin, Larry Schenkat, and Larkin Veigel. Flat surface reconstruction using minimal sonar readings. In *DARPA Image Understanding Workshop*, page to appear, 1996.

[Kleeman and Kuc, 1995] L. Kleeman and R. Kuc. An optimal sonar array for target localization and classification. *IEEE Trans. Robotics and Automation*, 14(4):pp. 295–318, August 1995.

[Kuc, 1990] R. Kuc. A spatial sampling criterion for sonar obstacle detection. *IEEE Trans. Pattern Analysis and Machine Intelligence*, 12(7):pp. 686–690, July 1990.

[Kuc, 1991] R. Kuc. A physically based navigation strategy for sonar guided vehicles. *Int. J. Robotics Research*, 10(2):pp. 75–87, April 1991.

[Leonard and Durrant-Whyte, 1991] John J. Leonard and Hugh F. Durrant-Whyte. Mobile robot localization by tracking geometric beacons. *IEEE Journal of Robotics and Automation*, 7(3):376–382, 1991.

[Matthies and Elfes, 1988] Larry Matthies and A. Elfes. Integration of sonar and stereo range data using a grid-based representation. In *IEEE Int. Conf. Robotics and Automation*, pages pp. 727–733, April 1988.

[Peremans *et al.*, 1993] Herbert Peremans, K. Audenaert, and Jan Van Campenhout. A high-resolution sensor based on tri-aural perception. *IEEE Trans. Robotics and Automation*, 9(1):pp. 36–48, February 1993.